Supplementary Information Material for:

Decoupling Ion Size from Electrochemistry: Cation-Size-Independent Accommodation of Li^+ to Cs^+ in an Amorphous Sulfonamide Coordination Polymer

Robert Markowski[1], Darsi Rambabu[1], Augustin Ramackers [1], and Alexandru Vlad[1,2] *

[1] *Institute of Condensed Matter and Nanosciences, Molecular Chemistry, Materials and Catalysis, Université catholique de Louvain, Louvain-la-Neuve B-1348, Belgium*

[2] *WEL Research Institute, avenue Pasteur, 6, 1300 Wavre, Belgium*

* *Corresponding author:* alexandru.vlad@uclouvain.be

Materials and methods

1,2,4,5-Benzenetetramine tetrahydrochloride (97.0%, Fluorochem), pyridine (Fisher Scientific), methanesulfonyl chloride (99.5%, Fisher scientific), anhydrous methanol (99.9%, Alfa Aesar), lithium methoxide (98%, Sigma Aldrich), anhydrous zinc (II) chloride (98%, Alfa Aesar), anhydrous calcium chloride (98%, Sigma Aldrich), anhydrous propylene carbonate (99.7%, Sigma Aldrich), lithium bis(trifluoromethanesulfonyl)imide (99+%, Solvionic) sodium bis(trifluoro methanesulfonyl)imide (99+%, Solvionic), potassium bis(trifluoromethanesulfonyl)imide (99+%, Solvionic), rubidium bis(trifluoromethanesulfonyl)imide (99+%, Solvionic), cesium bis(trifluoro methanesulfonyl)imide (99+%, Solvionic), were used as received. Coin cell assembly parts (stainless steel, SS-316), active carbon, conductive carbon and polytetrafluoroethylene (PTFE) were purchased from TOB New Energy Technology Co., Ltd. (Xiamen, China). The Glass fiber separator (GF/D) was purchased from Whatman. Active carbon fabric (ACC-5092-20) was purchased from Kynol. Li and Na metal chips (15.6 mm diameter) were purchased from Aotbattery, China.

Instrumentation

Fourier transform Infra-Red (FTIR) spectroscopy was performed on Agilent Technologies Cary 630 FTIR operated in ATR mode, in the wavenumber range from 4000 cm^{-1} to 650 cm^{-1}, and at a resolution of 4 cm^{-1} within 64 scans. Elemental analysis (CHNS) was done with Thermo Scientific™

FlashSmart™ Elemental Analyzer. Inductively coupled plasma-optical emission spectrometry (ICP-OES) analysis was performed on Perkin Elmer™ Avio220 max.

Assembly and testing of two-electrode coin cells

The electrochemical tests were carried out using 2025-type coin cells with a 13 mm diameter active carbon fabric used as counter and pseudo-reference electrode, and glass microfibre filter as the separator. The positive electrode composition was made by hand-grinding 50 % CP active material with 40 wt.% conductive carbon (Super P carbon, C-45) and 10 wt.% PTFE as a binder. The electrodes were assembled by applying the composite powder to the positive side of the coin cell case (CR 2032, AISI 316L stainless steel) and compacting with a stainless-steel disk. The typical active material loading was 1-2 mg, with areal loading of about 1.5-2 mg/cm^2. At room temperature, galvanostatic charge/discharge experiments were conducted using a Neware battery testing equipment. As electrolyte, 1.0 mol.L^{-1} MTFSI (M=Li$^+$, Na$^+$, K$^+$, Rb$^+$ and Cs$^+$) in PC was utilized. The water content of the prepared Li$^+$, Na$^+$, K$^+$, Rb$^+$ and Cs$^+$ electrolytes was generally below 20 ppm, as determined by Karl Fischer titration, Metrohm 899 Coulometer.

Assembly and testing of three-electrode cells

The assembly of the three-electrode cells was performed in an Ar-filled glovebox. Active carbon and a Ag wire were used as counter and pseudo-reference electrodes, respectively; and 1.0 mol L^{-1} MTFSI (M=Li$^+$, Na$^+$, K$^+$, Rb$^+$ and Cs$^+$) in PC as electrolyte. The working potential (*vs* Ag) of M_2-Zn-PTtSA positive electrodes was evaluated by galvanostatic charge-discharge using VMP galvanostat/potentiostat (Bio-Logic, France). The potential of the Ag pseudo-reference electrode was calibrated using cyclic voltammetry at a scan rate of 1 mV s^{-1}, in a three-electrode system, using a glassy carbon working electrode, a platinum counter electrode, and a Ag wire pseudo-reference electrode. The calibration was performed using 0.01 M ferrocene (as internal reference) with 1.0 mol L^{-1} MTFSI (M=Li$^+$, Na$^+$, K$^+$, Rb$^+$ and Cs$^+$) in PC as the supporting electrolyte.

Ex-situ FTIR measurements

For the *ex-situ* FTIR analysis the active materials were cycled at a rate of C/10 to reach the desired state of charge. Afterwards, the cells were disassembled, and the composite powder electrodes were collected in an argon-filled glove box. The powders were washed with THF and vacuum-dried at 80 °C.

The FTIR spectra were collected on Agilent Technologies Cary 630 FTIR operated in ATR mode inside an Ar-filled glove box, measured in the wavenumber range from 4000 cm^{-1} to 650 cm^{-1} at a resolution of 4 cm^{-1} with 64 scans.

Chemical Synthesis of Na_2-Zn-PTtSA

All manipulations were carried out in an argon-filled glovebox. A solution of Na_4-PTtSA was prepared by reacting H_4-PTtSA (225 mg, 0.5 mmol) and sodium methoxide (108 mg, 2 mmol) in anhydrous methanol (5 mL). A separate solution of $ZnCl_2$ was prepared by dissolving anhydrous zinc(II) chloride (68.1 mg, 0.5 mmol) in anhydrous methanol (3 mL). The two solutions were combined and stirred for 48 h. The resulting precipitate was collected by filtration and washed with methanol and diethyl ether. The solid was dried at 60 °C for 2 h, followed by further drying at 150 °C for 4 h. The yield was 92%. The elemental composition was confirmed by ICP-OES with respect to the metal content, giving a Na^+/Zn^{2+} ratio of 2.01.

Chemical Synthesis of Cs_2-Zn-PTtSA

All manipulations were carried out in an argon-filled glovebox. H_4-PTtSA (200 mg, 0.44 mmol, 1.0 equiv.) and lithium methoxide (66.8 mg, 1.76 mmol, 4.0 equiv.) were dissolved in anhydrous methanol (10 mL) in a 20 mL vial and stirred for 1 h. A solution of zinc(II) chloride in anhydrous methanol (1 mL) was then added dropwise, and the mixture was stirred for 24 h. Subsequently, cesium chloride (148.2 mg, 0.88 mmol, 2.0 equiv.) dissolved in anhydrous methanol (1 mL) was added dropwise, and the reaction was stirred for an additional 24 h. The mixture was centrifuged to separate the precipitate from the transparent supernatant. The precipitate was washed three times with anhydrous methanol and three times with anhydrous diethyl ether. The resulting powder was dried under vacuum at 120 °C for 14 h. The yield was 95%. The elemental composition was confirmed by ICP-OES with respect to the metal content, giving a Cs^+/Zn^{2+} ratio of 1.94.

Table S1. Concentration of Zn^{2+}, Ca^{2+}, and M^{+} (mol L^{-1}) measured in the solutions resulting from the digestion of M_2-Zn-PTtSA electrodes after five charge-discharge cycles. After complete digestion of the cycled electrodes, the concentration of each metal species in the resulting solutions was quantified by ICP-OES, and the corresponding values are reported in the table.

Material	Zn^{2+}	Ca^{2+}	M^{+}
Li_2-Zn-PTtSA	0.03686	0.00040	0.07189
Na_2-Zn-PTtsA	0.03657	0.00043	0.07147
K_2-Zn-PTtsA	0.02199	0.00038	0.04284
Rb_2-Zn-PTtSA	0.03690	0.00053	0.07184
Cs_2-Zn-PTtSA	0.03626	0.00057	0.07103

Table S2. Ca^{2+}/Zn^{2+} and M^{+}/Zn^{2+} atomic ratios in digested M_2–Zn–PTtSA electrodes after five charge–discharge cycles. This number corresponds to the atomic ratio, i.e., the number of Ca^{2+} atoms per Zn^{2+} atom and the number of M^{+} atoms per Zn^{2+} atom in the cycled electrodes, as calculated from ICP-EOS data analysis presented in **Table S1**.

Material	Ca^{2+}/Zn^{2+}	M^{+}/Zn^{2+}
Li_2-Zn-PTtSA	0.010	1.950
Na_2-Zn-PTtsA	0.011	1.954
K_2-Zn-PTtsA	0.017	1.947
Rb_2-Zn-PTtSA	0.014	1.946
Cs_2-Zn-PTtSA	0.015	1.958

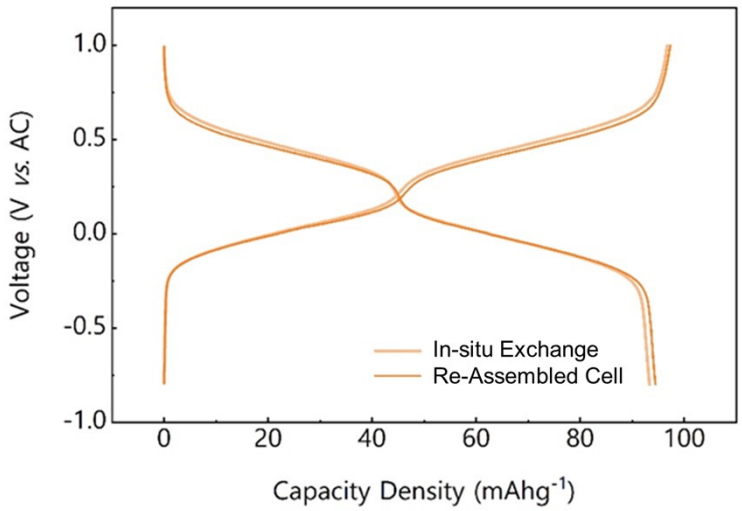

Figure S1. Comparison of Cs^+ storage in two positive electrode material configurations: (i) direct cycling of Ca-Zn-PTtSA in 1 M CsTFSI/PC (marked as *In-situ* Exchange), and (ii) reassembled cell using a charged and washed ⬚–Zn–PTtSA electrode (after complete Ca extraction; marked as Re-Assembled Cell) in 1 mol L^{-1} CsTFSI/PC.

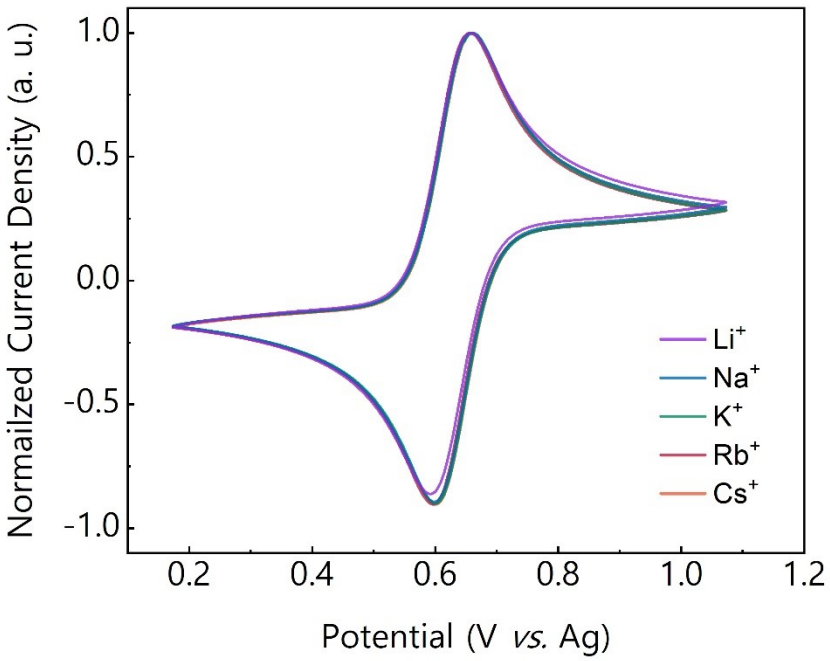

Figure S2. Cyclic voltammograms of the Fc^{+}/Fc redox couple *vs* Ag wire pseudo-reference electrode in various 1 mol L^{-1} MTFSI in PC electrolytes.

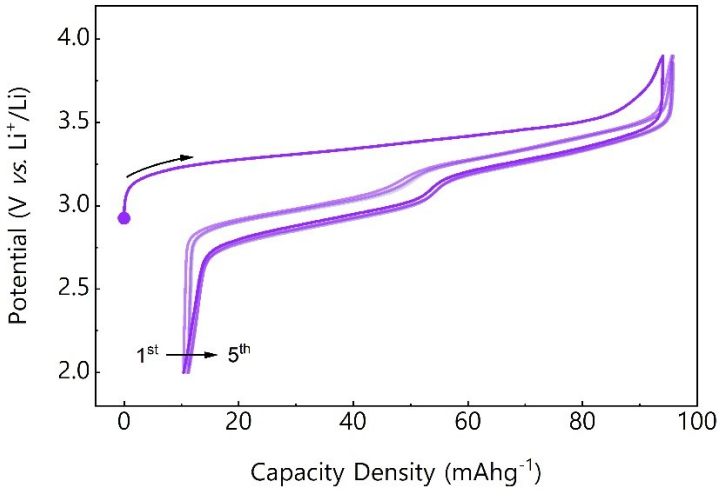

Figure S3. Galvanostatic charge-discharge profile of Ca-Zn-PTtSA electrode cycled in a Li metal half-cell configuration with 1 mol L^{-1} LiTFSI in PC.

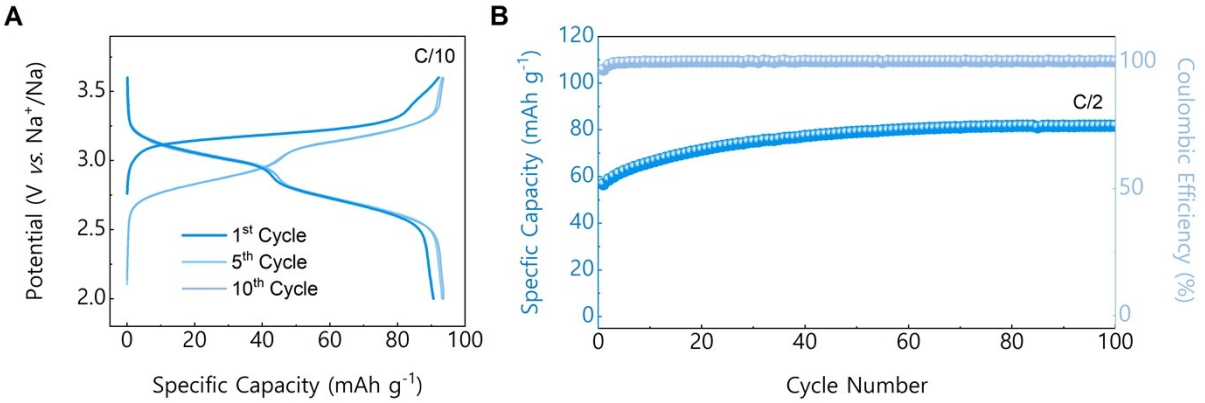

Figure S4. (**A**) Galvanostatic charge-discharge profile of Ca-Zn-PTtSA electrode cycled in a Na metal half-cell configuration with 1 mol L^{-1} NaTFSI in PC, at a current density of 10 mA g^{-1}. (**B**) Evolution of the specific discharge capacity and columbic efficiency of Ca-Zn-PTtSA electrode cycled in a Na metal half-cell configuration with 1 mol L^{-1} NaTFSI in PC, at a current density of 50 mA g^{-1}.

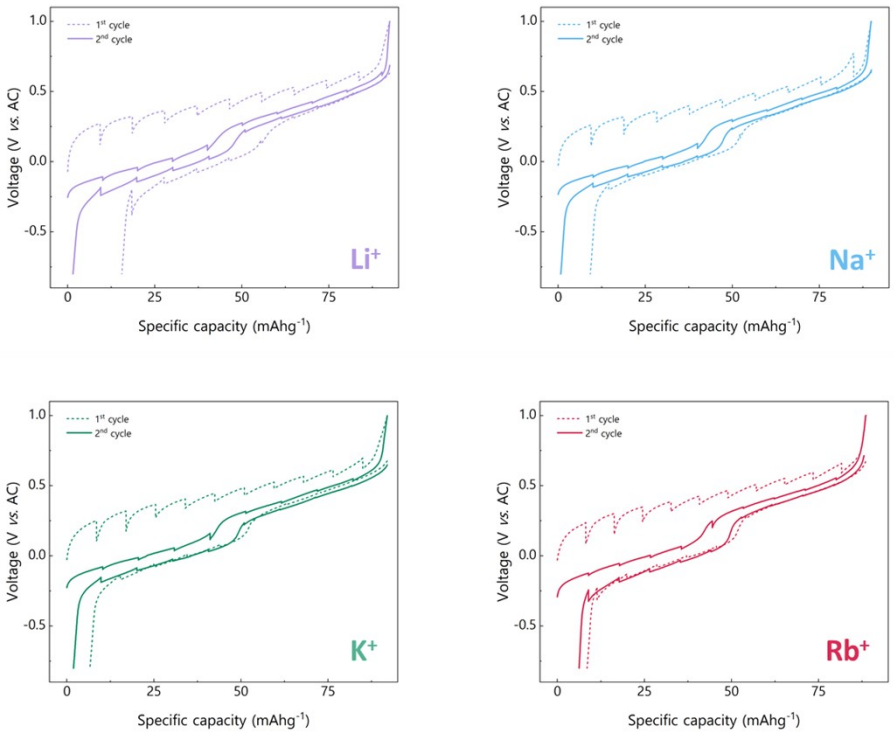

Figure S5. GITT curves of Ca-Zn-PTtSA electrodes during the first two galvanostatic charge-discharge cycles acquired at a current density of 10 mAg^{-1} in corresponding 1 mol L^{-1} MTFSI (M^+ = Li^+, Na^+, K^+, Rb^+) in PC electrolyte; with 5 h OCV relaxation period following each galvanostatic charge collection or injection for a duration of 1 h.

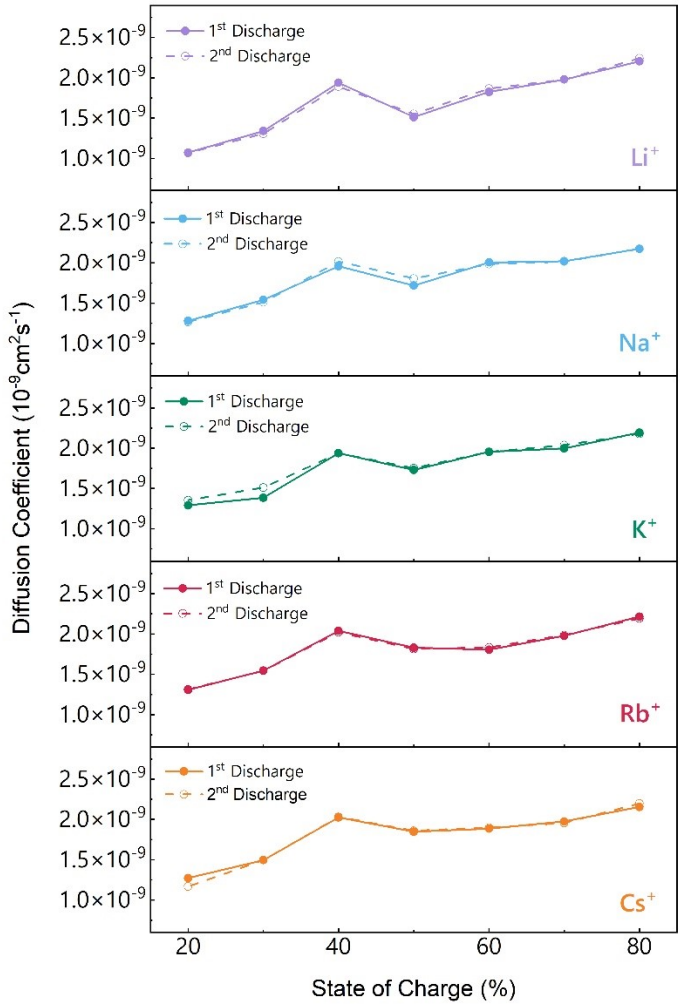

Figure S6. Calculated diffusion coefficient of $Li^+/Na^+/K^+/Rb^+/Cs^+$ in the corresponding M_2-Zn-PTtSA positive electrode materials during the 1st and 2nd discharge process.

The diffusion coefficient D was calculated according to the equation:

$$D = \frac{4}{\pi\tau}(m_B V_m / M_B S)^2 (\Delta E_s / \Delta E_\tau)^2$$

Where τ is duration of the galvanostatic discharge/charge step, m_B, M_B and V_m refer to the active mass, the molar mass, and the molar volume. S is the geometric surface area of the electrode, ΔE_s is the change of OCV values between two subsequent charge inject steps and ΔE_τ is the voltage variation during a current pulse.

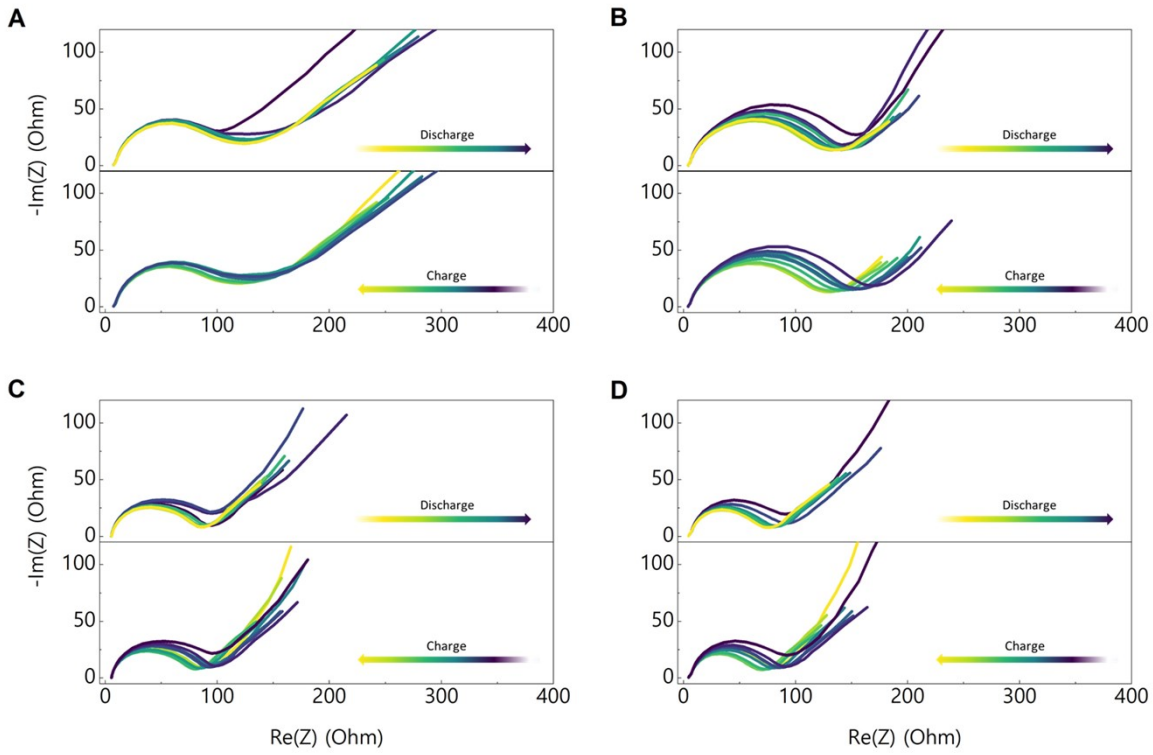

Figure S7. In situ electrochemical impedance spectroscopy (EIS) collected during the second charge and discharge of the Ca-Zn-PTtSA electrode cycled in 1 mol L^{-1} (A) LiTFSI, (B) NaTFSI, (C) RbTFSI and (D) CsTFSI in propylene carbonate as electrolyte, at a current density of 10 mA g-1. The EIS spectrum was recorded after each electrochemical step, consisting of 1 h of charge or discharge followed by a 1 h rest period. The only noticeable trend is that the resistance variation during Li^+ storage is less pronounced than for the other cations. This behavior may be related to the smaller ionic radius of Li^+, which is expected to induce less pronounced structural perturbations within the polymer framework, leading to smaller changes in electronic conductivity. Nevertheless, further advanced analyses are required to determine the exact origin of this.

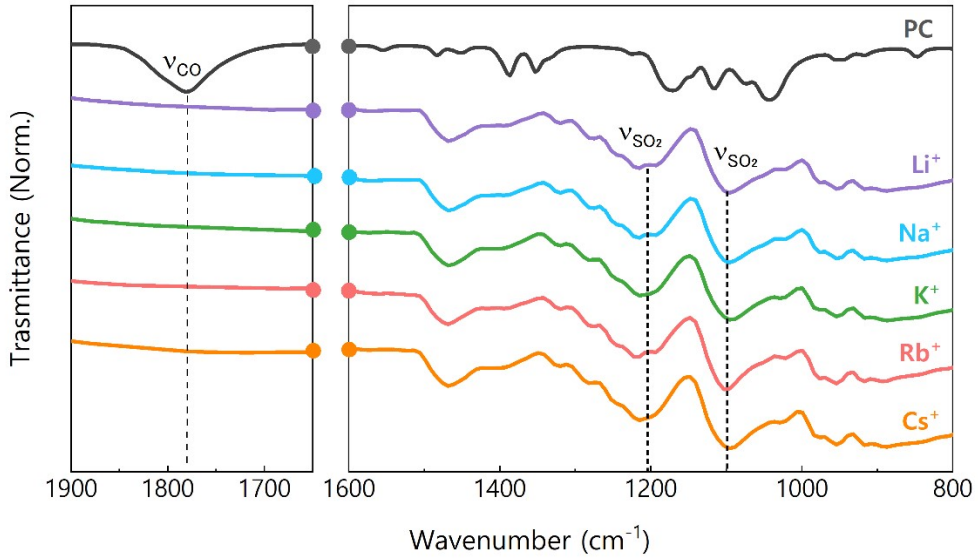

Figure S8. Ex-situ FTIR spectra of electrochemically reduced Li_2-Zn-PTtSA, Na_2-Zn-PTtSA, K_2-Zn-PTtSA, Rb_2-Zn-PTtSA, and Cs_2-Zn-PTtSA phases. Propylene carbonate spectra is overlayed for comparison and identification of specific bands.

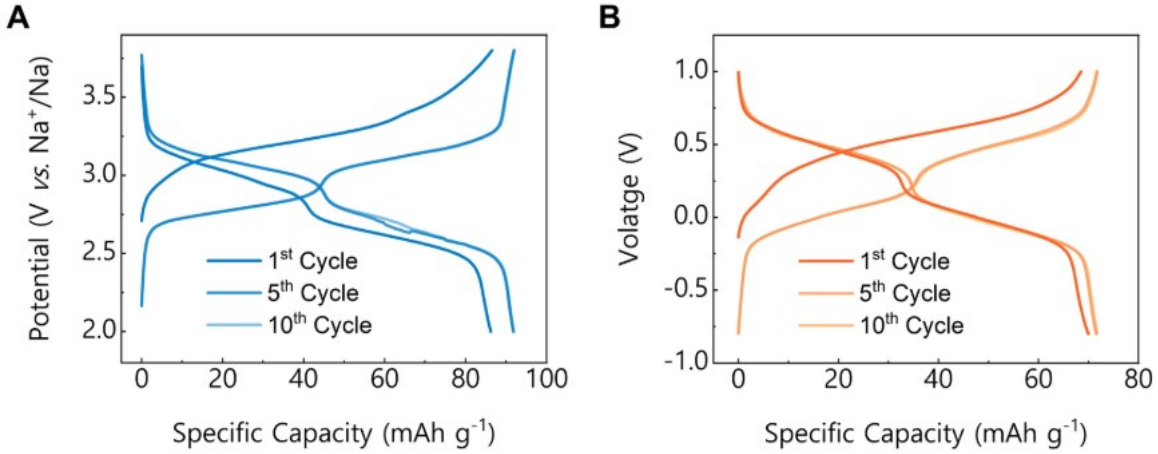

Figure S9. Galvanostatic charge-discharge profiles at the 1st, 5th and 10th cycle for (A) Na_2-Zn-PTtSA electrode cycled in a Na metal half-cell configuration with 1 mol L^{-1} NaTFSI in PC at a current density of 9 mA g^{-1} (C/10), and (B) Cs_2-Zn-PTtSA a activated carbon two-electrode cell configuration with 1 mol L^{-1} CsTFSI in PC at a current density of 7 mA g^{-1} (C/10).